

## Imaging the Elastic Nanostructure of Ge Islands by Ultrasonic Force Microscopy

Oleg V. Kolosov, Martin R. Castell, Chris D. Marsh, and G. Andrew D. Briggs

*Department of Materials, University of Oxford, Parks Road, Oxford, OX1 3PH, England*

T. I. Kamins and R. Stanley Williams

*Hewlett-Packard Laboratories, 3500 Deer Creek Road, Palo Alto, California 94304-1392*

(Received 25 September 1997)

The structure of nanometer-sized strained Ge islands epitaxially grown on a Si substrate was studied using ultrasonic force microscopy (UFM), which combines the sensitivity to elastic structure of acoustic microscopy with the nanoscale spatial resolution of atomic force microscopy. UFM not only images the local surface elasticity variations between the Ge dots and the substrate with a spatial resolution of about 5 nm, but is also capable of detecting the strain variation across the dot, via the modification of the local stiffness. [S0031-9007(98)06741-6]

PACS numbers: 81.40.Jj, 43.35.+d, 61.16.Ch

Successes in nanotechnology aimed at the controlled growth of nanoscale structures provide a significant challenge to the existing methods of surface characterization. The physical properties of such structures are intrinsically heterogeneous and vary strongly over distances of the order of several nanometers. Local elastic properties, particularly, play an important role in strained low dimensional heterostructures, strongly affecting their electrical properties and influencing growth and the mechanical stability of such structures [1,2].

Whereas imaging of local electronic properties of nanostructures is relatively well developed (e.g., by electron or scanning tunneling microscopy [3–5]), the physical principles of nanoscale imaging of elastic properties are at an elementary stage. Established methods of microstructural characterization of elastic properties possess either high sensitivity to elastic properties but insufficient spatial resolution (e.g., acoustic microscopy [6–8] or nanoindentation [9]), or adequate resolution but no sensitivity to elastic properties of such rigid materials as semiconductors [e.g., atomic force microscopy (AFM) [10,11] or force modulation microscopy [12]]. The ideal solution would be to combine the advantages of these two approaches, e.g., by detecting ultrasound with an AFM tip. Unfortunately, the AFM cantilever response to ultrasonic vibration in the 1–100 MHz frequency range is very small [13].

Nevertheless, it was recently demonstrated that this problem could be solved using nonlinear detection of ultrasonic vibration [14], which is the core principle of ultrasonic force microscopy (UFM) [15]. UFM exploits the extreme dynamic stiffness of the cantilever [which exceeds the low-frequency (LF) stiffness by a factor of  $10^2$ – $10^4$ ] by forcing the vibrating sample to elastically “indent” itself against the dynamically frozen cantilever tip. Owing to the sharp nonlinearity of the tip-surface force-versus-separation dependence  $F(z)$ , such indentation, repeated with ultrasonic frequency, reveals itself as an additional constant force acting on the cantilever and is

easily detected with an extremely force sensitive (at LF) AFM cantilever.

Studies have been reported that show that HF vibration of the cantilever, although relatively weak, could also be detected using a special detection system [16–18] and applied to probe the elastic properties of stiff materials. Nevertheless, these systems inevitably compromise sensitivity to material properties (demanding higher rigidity of the cantilever) with sensitivity to the tip-surface interaction force (demanding lower rigidity) [17]. UFM achieves a reasonable compromise in an unusual way by separating the two cantilever functions (indentation and force detection) in the frequency domain.

In this Letter we report new results on direct imaging using the novel UFM technique, of the local elastic properties of a group IV semiconductor nanostructure system [Ge dots on a Si (001) substrate] with nanoscale resolution. The UFM experiments were complemented by scanning electron microscopy (SEM) and transmission electron microscopy (TEM) studies.

Ge dots were grown on a standard (100) Si substrate following the procedure described in detail elsewhere [19]. The growth was performed in an ambient pressure of 10 Torr at a temperature of about 600 °C. Pseudomorphic growth was observed at thicknesses below approximately 3.5 ML (calibrated by Rutherford back scattering) of Ge resulting in a topographically flat and smooth surface. It is only after this initial flat Ge layer is deposited that the islands start to appear. In this work we will report studies of a sample with 11 equivalent monolayers (including the material in the dots and in the “wetting layer” between the dots) of Ge, containing islands with a narrow size distribution.

The easiest way to realize the UFM mode for imaging elastic properties of Ge islands was to modify a standard commercial AFM [20]. The modification is relatively simple [14,15], and consists of applying an amplitude-modulated ultrasonic vibration ( $\sim 3$  MHz) which is

detected as a nonlinear force response (Fig. 1). Our setup enabled direct observation of the dependence of the cantilever deflection  $z_c$  on the ultrasonic amplitude  $a_u$  using a digital oscilloscope. A ramp modulation envelope ( $\sim 2\text{--}3$  kHz) was combined with lock-in detection to be sensitive to changes in the ultrasonic amplitude at which the inflection in Fig. 1(b) occurred, which depends on the local materials properties [21]. An image of this UFM response could be recorded simultaneously with a standard topography image.

Topographical AFM images of Ge dots [Fig. 2(a)] revealed nearly identical islands of approximately 15 nm height and 60 nm width [bright elliptical areas in Fig. 2(a), the elongation is caused by the piezoscanner distortion] with a smooth surface, consistent with AFM observations of similar structures reported elsewhere [19]. The same  $400 \times 400$  nm<sup>2</sup> area of the sample was investigated by UFM. The Ge dots were clearly seen in the UFM images, with the UFM signal from the dot [darker regions in Fig. 2(c)] noticeably smaller than that from the Si substrate. The UFM elasticity profile [Fig. 2(d)] of the dots appeared to be relatively flat on the top (except the central area of the dot, to be discussed below). All these features are exactly what one would expect from UFM contrast of softer Ge (Young modulus,  $E_{\text{Ge}} = 121$  GPa) on more rigid Si ( $E_{\text{Si}} = 164$  GPa) [15]. The bright "halo" around the dot is, effectively, an edge effect in areas where the rounded AFM tip simultaneously touches the protruding dot and the substrate, increasing the effective tip-surface contact stiffness (and UFM response). Nevertheless, this halo allowed us to estimate an upper limit of the contact region (and, therefore, the UFM resolution) to be about 5–10 nm. We also noted slight faceting of the dot edges in contact with the substrate along  $\langle 100 \rangle$ -type directions and some elastic heterogeneity of the Ge wetting layer. UFM

images were very stable and showed no signs of deterioration after hours of operation in the UFM mode.

These images show that direct observation by UFM of local elastic properties of nanoscale quantum structures with spatial resolution of the order of several nm is possible, as anticipated. Detailed observation shows an unexpected round structure in the center of the Ge dot of approximately 20 nm in diameter. It was clearly seen in the UFM images [Figs. 2(c), 2(d)] and exhibits an elastic contrast with effective elastic modulus intermediate between Si and Ge. Successive experiments (using different tips, forces, etc.) confirmed that UFM images consistently reveal a hole in the center of the Ge dot, with no sign of it in the AFM topography images. The next step was to understand what these holes could be, in particular, applying other imaging techniques such as SEM and TEM.

The SEM images [Figs. 3(a), 3(b)] were acquired in a Hitachi S900 field emission SEM using the secondary electron (SE) imaging mode. All the Ge islands analogous to the ones observed by UFM appeared as bright dots, with evidence of faceting, and distinct dark centers and less profound darker crosses in  $\langle 110 \rangle$  directions. A  $60^\circ$  tilted image [Fig. 3(b)] highlights topographical contrast and dot faceting.

One could think of several possibilities for the SEM contrast of the hole in the Ge dot, namely: (a) peculiarities in *topography* (e.g., an extended flat region on the top of the dot), (b) *material composition*, (c) *electron channeling*, and (d) *variation of electron band structure* [22]. As AFM topography of the dot and a  $60^\circ$  tilted SEM image (enhancing topographical features) revealed an essentially smooth surface of the dots, we believe that *topography* was not the cause of the hole contrast. *Electron channeling* was also rejected because the dark

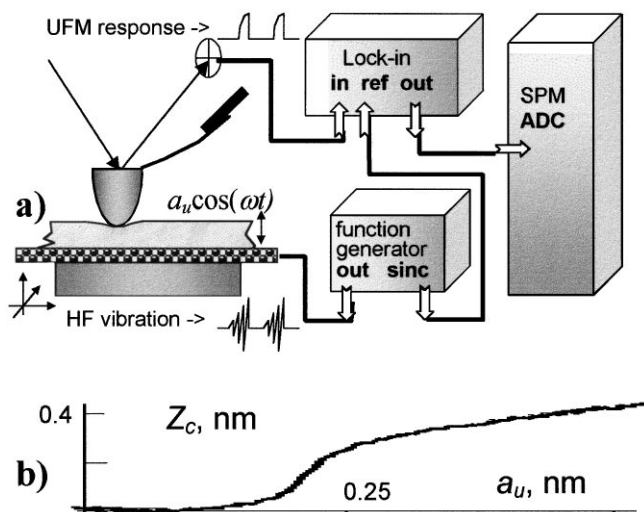


FIG. 1. (a) Experimental setup of ultrasonic force microscope (UFM); (b) typical experimental dependence of UFM response (cantilever deflection  $z_c$ ) on ultrasonic vibration amplitude  $a_u$ .

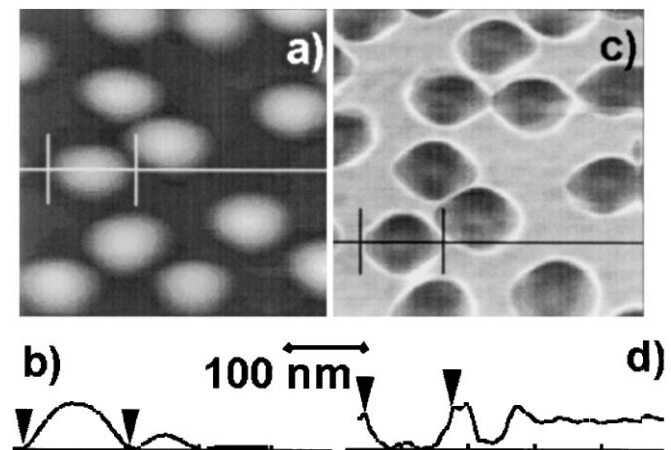


FIG. 2. Topography (a) and UFM image (c) of area containing Ge dots on a Si substrate and corresponding topography (b) and UFM (d) profiles across the same Ge island [triangles on the profile, thin line in (a), (c)]. A round structure in the center of the dot is detected in the UFM, while the topography profile of the dot is perfectly smooth. Height of the dots in (a), (c) is about 15 nm.

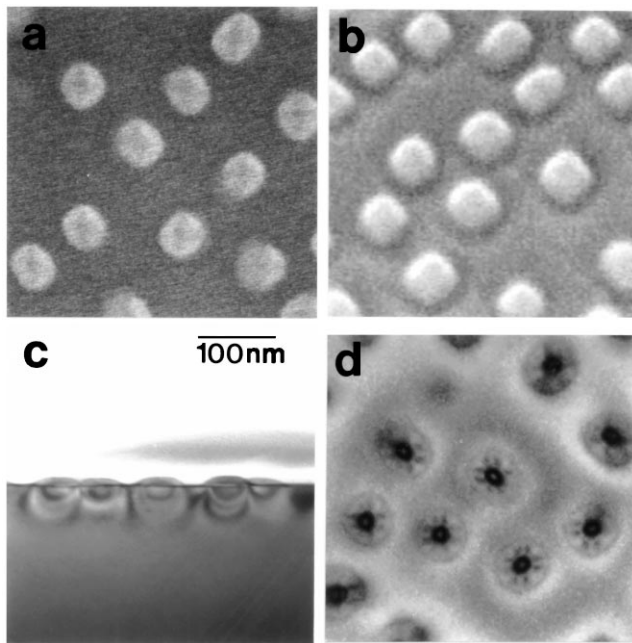


FIG. 3. Plan view (a) (20 keV, secondary electrons) and 60° tilted (b) (1 keV, secondary electrons, with aspect ratio compensation) SEM images of Ge dots. TEM cross-section (c) and plan view (d) images. The structure in the center of the dots analogous to that observed in the UFM image (Fig. 2) is clearly visible. Note the strain caused by the dots in the Si substrate (c). The edges of images (a), (b), and (d) are parallel to  $\langle 110 \rangle$  directions.

centers were still present after the sample was tilted by up to 10°. *Material composition* (e.g., due to the presence of Si in the dot center) was relatively unlikely because the low temperature restricts solid state diffusion, and the strain gradient and segregation drive Ge, rather than Si, toward the top of the island. At the same time the *variation of electron band structure* because of strain appears quite plausible, as (1) it has recently been reported that a highly compressed (due to the 4% Si/Ge lattice mismatch) Ge dot can be relatively relaxed in its center near the top [23], which (2) should be observed in SE imaging as a darker central region, according to recent studies on strained SiGe layers [24].

TEM [25] two-beam ( $g_{400}$ ) plan-view and cross-section images showed that the Ge dot and the Si substrate under the dot were strained [Fig. 3(c)]. At the same time in plan view, higher resolution multibeam images at the (100) zone axis [Fig. 3(d)] showed a very clear structure in the center of each Ge dot of approximately the same size as the hole in the UFM images, but with a ringlike shape. Crosslike structures along  $\langle 110 \rangle$  directions (as in the SEM images) were also apparent. Such TEM contrast could most probably be attributed to the tilt of the crystalline planes because of the strain. That would produce the central ring and [because of the fourfold symmetry of the strain for the (001) surface [26]] crosses. The cross-sectional TEM images also

confirmed the absence of relaxation of our Ge/Si system by dislocations.

Together SEM and TEM indicated that the most plausible cause for the hole in the epitaxial Ge dot on the Si substrate is inhomogeneous strain across the dot, strongest at its perimeter and relaxed near the top of the dot center. This raised the question: What physical mechanisms might give rise to strain contrast in UFM? In order to answer this question it is useful to analyze UFM contrast for the Si-Ge system.

As reported elsewhere [14], the AFM cantilever response to the HF sample vibration of amplitude  $a_u$  can be described by the introduction of a new force-versus-separation dependence  $F_m(z)$ , derived from the original  $F(z)$  dependence by averaging over a vibration period  $T$  [14,27].

$$F_m(z) = \int_0^T F \left[ z - a_u \cos \left( 2\pi \frac{t}{T} \right) \right] dt. \quad (1)$$

This reduces the problem of the UFM response to the well-known force balance equation in AFM [14,27].

The choice of a continuum mechanics description of the tip-surface force interaction  $F(z)$  depends on geometry, elastic properties, and surface energy [28]. An approximation that lends itself to analytical modeling is the Johnson-Kendall-Roberts (JKR) model [29]. In dimensionless units of force  $F = F/\pi WR$  and displacement  $z = z/(\pi^2 W^2 R/K^2)^{1/3}$  (where  $R$  is the tip radius,  $W$  is the adhesion energy, and  $K = (4/3)/\{(1 - \nu_t^2)/E_t + (1 - \nu_s^2)/E_s\}$  is the effective elasticity of the tip-surface contact, depending on  $(E_s, \nu_s)$  and  $(E_t, \nu_t)$ , the Young's moduli and Poisson ratios of the sample and tip, respectively) JKR gives  $z = d^2 - (8d/3)^{1/2}$ , where  $d = \{F + 3 + (6F + 9)\}^{1/3}$ . The inherent hysteresis between the approach and retraction force dependencies  $F(z)$  in the JKR model was taken into account while calculating the integral (1).

Further calculation of the UFM response is straightforward. We used literature values of Si and Ge elastic moduli ( $E_{Si} = 164$  GPa,  $E_{Ge} = 121$  GPa) [6], the surface energy in an ambient environment ( $W \approx 1$  N/m) [30], and the manufacturer's data for tip radius ( $\approx 10^{-8}$  m) [20]. The changes in the elastic moduli for 4% strained Ge were estimated using third order elastic moduli [31], which gave a decrease of approximately (10–20)% for the Ge elastic moduli of compressed Ge.

The calculated UFM response is plotted in Fig. 4(a). It reveals similar qualitative features as the experimental curve [Fig. 1(b)]. The UFM response for unstrained Si and Ge [curves *i* and *ii* in Fig. 4(a)] was distinctly different, with the Ge response “delayed” and smaller compared with that of Si. Therefore we could expect a smaller UFM output for Ge, confirming the possibility of directly mapping the elasticity of Si-Ge nanostructures. Moreover, the calculated UFM response of strained Ge (curve *iii*) was noticeably smaller than that from relaxed Ge [curves *ii*, Fig. 4(a)]. A simulated UFM cross-section of the dot

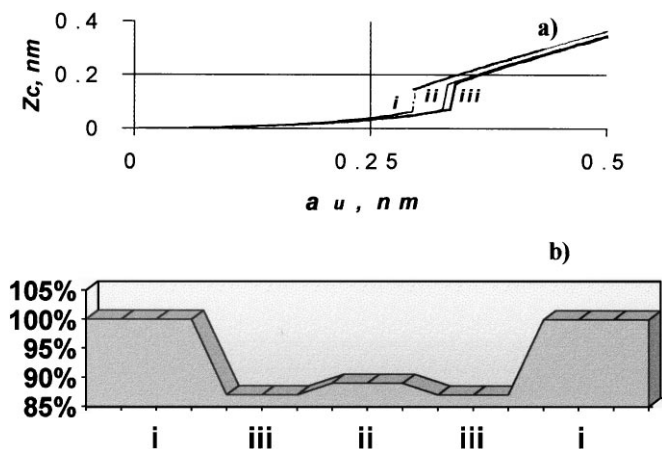


FIG. 4. (a) Calculated theoretical dependencies of cantilever response  $z_c$  vs ultrasonic vibration  $a_u$  for unstrained Si (i) and Ge (ii) and for strained Ge (iii). (b) A schematic representation of the simulated UFM profile across a Ge dot on a Si substrate containing areas of Si, Ge, and strained Ge [vertical scale in (b) is normalized to the UFM signal from the Si area].

containing all three areas (Si, strained Ge with relaxed Ge in the center) in Fig. 4(b) shows great similarity with the experimental UFM cross-section of the dot [Fig. 2(d)].

In conclusion, ultrasonic force microscopy (UFM) was successfully applied to imaging local elastic properties of nanometer scale epitaxial Ge dots on a Si (001) substrate with a lateral resolution of elastic properties better than 10 nm. UFM sensitivity is sufficient for the detection of local strain variations in such structures (revealing itself through the variation of stiffness) provided other sources of the contrast (e.g., material composition, topography, etc.) are taken into account. The UFM contrast of the elastically relaxed area at the center of the dot with a diameter of approximately 1/3 of the dot was consistent with subsequent SEM and TEM measurements. We believe that the novel UFM approach opens a unique opportunity for studies of quantum nanostructures, particularly for mapping their local elasticity and strain, which are essential parameters affecting both applications and manufacturing of such structures.

We would like to acknowledge David Bottomley, Roger Booker, Franco Dinelli, Teresa Cuberes, and Doug Perovic for useful discussions. We are also grateful to the Paul Instrument Fund and EPSRC for the enthusiastic support of the UFM development and to Wolfson College, Oxford and CEC AFAM Network for their support.

[1] P.M. Petroff and G. Medeiros-Ribeiro, MRS Bull. **21**, 50 (1996).

- [2] D. J. Eaglesham and M. Cerullo, Phys. Rev. Lett. **64**, 1943 (1990).
- [3] D. Leonard *et al.*, Appl. Phys. Lett. **63**, 3203 (1993).
- [4] D. Leonard *et al.*, J. Vac. Sci. Technol. B **12**, 1063 (1994).
- [5] O. Schoenfeld *et al.*, Solid State Electron. **40**, 605 (1996).
- [6] A. Briggs, *Acoustic Microscopy* (Clarendon Press, Oxford, 1992).
- [7] O. Kolosov, M. Suzuki, and K. Yamanaka, J. Appl. Phys. **74**, 6407 (1993).
- [8] A. Briggs and O. Kolosov, MRS Bull. **21**, 30 (1996).
- [9] M.R. Castell, M.G. Walls, and A. Howie, Ultramicroscopy **42-44**, 1490 (1992).
- [10] G. Binnig, C.F. Quate, and C. Gerber, Phys. Rev. Lett. **56**, 930 (1986).
- [11] C. C. W. Martin and H. K. Wickramasinghe, J. Appl. Phys. **61**, 4723 (1987).
- [12] P. Maivald *et al.*, Nanotechnology **2**, 103 (1991).
- [13] S. Hirschorn, U. Rabe, and W. Arnold, Nanotechnology **8**, 57 (1997).
- [14] O. Kolosov and K. Yamanaka, Jpn. J. Appl. Phys. **32**, L1095 (1993).
- [15] O. Kolosov *et al.*, in *Nanostructures & Quantum Effects*, edited by H. Sakaki and H. Noge (Springer-Verlag, Berlin, 1994), Vol. 31, p. 349.
- [16] U. Rabe and W. Arnold, Appl. Phys. Lett. **64**, 1493 (1994).
- [17] N. A. Burnham *et al.*, J. Vac. Sci. Technol. B **14**, 1308 (1996).
- [18] K. Yamanaka and S. Nakano, Jpn. J. Appl. Phys. **35**, 3787 (1996).
- [19] T. I. Kamins *et al.*, J. Appl. Phys. **81**, 211 (1997).
- [20] CP (Multiprobe SPM, PSI).
- [21] F. Dinelli *et al.*, Appl. Phys. Lett. **71**, 1177 (1997).
- [22] D. D. Perovic *et al.*, Ultramicroscopy **58**, 104 (1995).
- [23] D. J. Eaglesham and R. Hull, Mater. Sci. Eng. **B30**, 197 (1995).
- [24] M. R. Castell, D. D. Perovic, and H. Lafontaine, Ultramicroscopy **69**, 279 (1997).
- [25] CM-20 (Philips).
- [26] D. J. Bottomley and P. Fons, J. Cryst. Growth **160**, 406 (1996).
- [27] D. Sarid and V. Elings, J. Vac. Sci. Technol. B **9**, 992 (1991).
- [28] D. Maugis and M. Barguins, J. Phys. D **11**, 1989 (1978).
- [29] K. L. Johnson, K. Kendall, and A. D. Roberts, Proc. R. Soc. London A **324**, 301 (1971).
- [30] J. N. Israelachvili and R. M. Pashley, Nature (London) **306**, 259 (1983).
- [31] Z. Sklar *et al.*, in *Advances in Acoustic Microscopy*, edited by A. Briggs (Plenum Press, New York, 1995), Vol. 1, p. 209.